Supplementary Materials: Preparation of Multicomponent Biocomposites and Characterization of their Physicochemical and Mechanical Properties

Yuriy A. Anisimov [1], Duncan E. Cree [2,*] and Lee D. Wilson [1,*]

[1] Department of Chemistry, University of Saskatchewan, Saskatoon, SK. S7N 5C9, Canada; iaa365@mail.usask.ca
[2] Department of Mechanical Engineering, University of Saskatchewan, Saskatoon, SK. S7N 5A9, Canada
* Correspondence: duncan.cree@usask.ca (D.E.C.); lee.wilson@usask.ca (L.D.W.); Tel.: +1-306-966-3244 (D.E.C.); +1-306-966-2961 (L.D.W.)

Table S1. List of shorthand notation used in this study.

Abbreviation	Compound	CHT, wt. %	PANI, wt. %	PVA, wt. %
CHT	chitosan	100	0	0
PANI	polyaniline	0	100	0
PVA	polyvinyl alcohol	0	0	100
APS	ammonium persulfate		polymerization initiator	
CHP25	binary composite	25	75	0
CHP50	binary composite	50	50	0
CHP75	binary composite	75	25	0
CHP25-PVA*	ternary composite	25	75	70**
CHP50-PVA	ternary composite	50	50	70**
CHP75-PVA	ternary composite	75	25	70**
CHP25-PVA50	ternary composite	25	75	50***
CHP50-PVA50	ternary composite	50	50	50***
CHP75-PVA50	ternary composite	75	25	50***
MB	methylene blue		dye for adsorption study	
FL	fluorescein		dye for adsorption study	

*CHP##-PVA is denoted as CHP##-PVA70, in order to highlight the content of PVA; **70% PVA and 30% CHP; ***50% PVA and 50% CHP; Acid-doped samples were denoted by the mark "doped" in this work

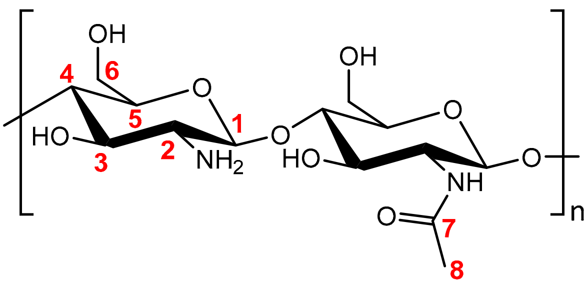

Figure S1. Numbering assignment scheme of chitosan ^{13}carbon atoms [1].

Table S2. FTIR bands of PANI-CHT-PVA composites.

Wavenumber (cm^{-1})	Assignment	Polymer Material
3259-3276 (3266)*	Hydrogen bonding N–H stretching	PANI
2937-2945 (2946)*	C–H from the alkyl groups	PVA
2907-2910 (2917)*	C–H symmetric stretching	CHT
1660 (1655)*	C=O stretching of amide	CHT
1588 (1586)*	Quinoid (Q) ring stretching	PANI
1545 (1543)*	N–H bending of amide	CHT
1495-1500 (1511)*	Benzenoid (B) ring stretching	PANI
1443-1446 (1445)*	C=C stretching of aromatic ring/N=N stretching	PANI
1428 (1427)*	stretching and bending vibrations of $-CH_2$	CHT
1417 (1413)*	Phenazine ring stretching	PANI
1376-1378 (1378)*	C–N stretching in QBQ units	PANI
1316 (1315)*	stretching and bending vibrations of –OH	CHT
1303-1308 (1302)*	ν(C–N) of secondary aromatic amine	PANI
1236-1239 (1240)*	ν(C–N) BBB unit	PANI
1164-1166 (1160)*	B–NH–B/δ(C–H)	PANI
1139-1141 (1143)*	C–O (crystallinity)	PVA
1069-1086 (1061)*	C–O stretching	PVA
1034 (1026)*	C–O stretching	CHT
827-835 (827)*	γ(C–H) (1,4-disubstituted ring)/Q ring deformation	PANI

*Literature values obtained from Ref. [2–5]

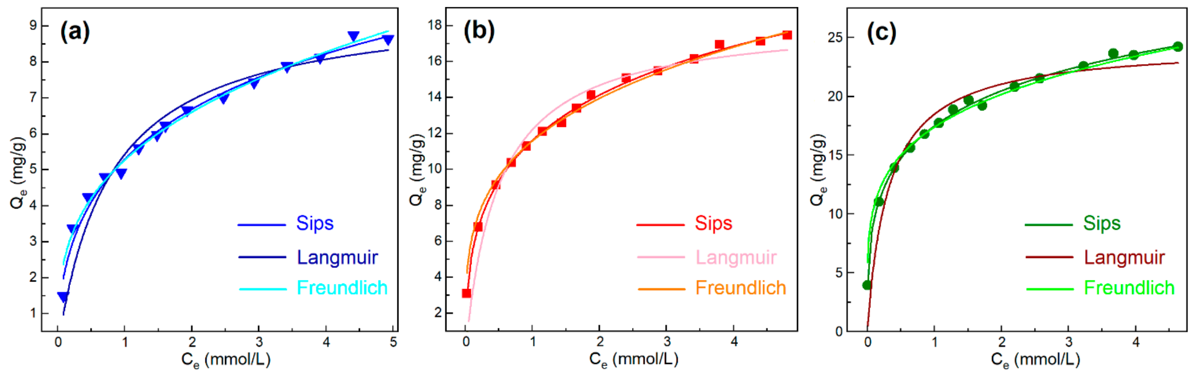

Figure S2. Fitting lines for (**a**) CHP25-PVA, (**b**) CHP50-PVA and (**c**) CHP75-PVA MB equilibrium uptake according to the various isotherm models. The error bars were determined using OriginLab 2019 software (see Table S3).

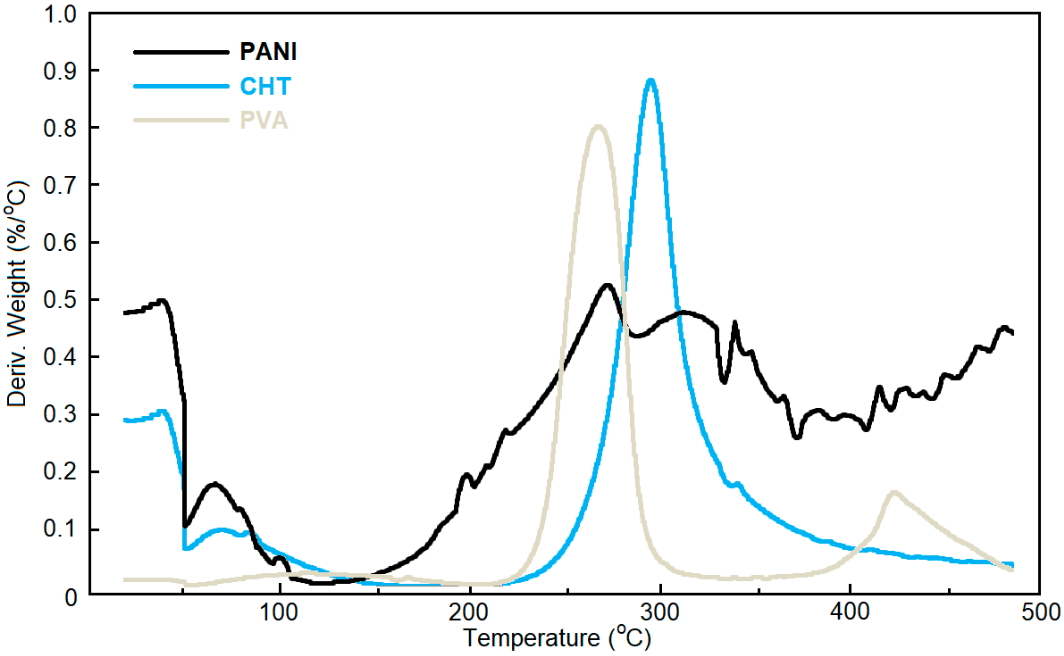

Figure S3. Thermogravimetry profiles of pristine components – PANI, CHT and PVA.

Table S3. Error bars for the adsorption experiments shown in Figure S2.

Sample	**Model / Parameters**	**Sips**	**Langmuir**	**Freundlich**
	Equation	$y = \frac{q(kx)^n}{1+(kx)^n}$	$y = \frac{qkx}{1+kx}$	$y = kx^{\frac{1}{n}}$
	Plot	$q_e = f(C_e)$	$q_e = f(C_e)$	$q_e = f(C_e)$
CHP25-PVA	q	19.112 ± 6.271	9.6414 ± 0.0302	—
	k	0.38222 ± 0.17865	1.2839 ± 0.0155	5.2642 ± 0.0179
	n	0.49157 ± 0.07528	—	3.0656 ± 0.0286
	Reduced Chi-Sqr	0.05777	0.07961	0.14234
	R-Square (COD)	0.98829	0.96879	0.94544
	Adj. R-Square	0.98633	0.96876	0.94538
CHP50-PVA	q	37.785 ± 4.132	18.396 ± 0.690	—
	k	0.44359 ± 0.07228	1.9719 ± 0.3190	11.585 ± 0.036
	n	0.42989 ± 0.02335	—	3.7293 ± 0.0392
	Reduced Chi-Sqr	0.03039	0.95926	0.63602
	R-Square (COD)	0.99846	0.94718	0.92940
	Adj. R-Square	0.99820	0.94312	0.92933
CHP75-PVA	q	51.542 ± 6.174	24.413 ± 0.870	—
	k	0.51174 ± 0.09540	3.0945 ± 0.5700	17.358 ± 0.049

n	0.36176 ± 0.02254	—	4.6487 ± 0.0571
Reduced Chi-Sqr	0.07016	2.1091	1.2815
R-Square (COD)	0.99798	0.93407	0.90318
Adj. R-Square	0.99764	0.92900	0.90308

Table S4. Mean densities of polymer composite materials based on geometric volume determination* of the film**.

Sample	Experimental Density, g/cm^3	Theoretical Density***, g/cm^3
CHP25-PVA	1.03 ± 0.03	1.20
CHP50-PVA	0.83 ± 0.06	1.14
CHP75-PVA	0.64 ± 0.03	1.08

*Geometric volume determination was conducted by digital caliper with the systematic error ±0.0025 cm. However, the random errors of the experiment are nearly 10-fold higher and therefore the instrumental error could be neglected. Sample weights were measured with an analytical balance with ±0.00001 g precision. Therefore, the error contribution to the overall density is negligibly small. **This method does not account for the porosity of samples directly; however, data was averaged over 15 samples that reveal a clear trend, where *greater chitosan content results in lower density*. A lower density indicates a more porous material. ***Theoretical density was calculated based on the rule of mixtures formula (Equation (S1)):

$$\rho = \frac{\rho_1 \rho_2 \rho_3}{\omega_1 \rho_2 \rho_3 + \omega_2 \rho_1 \rho_3 + \omega_3 \rho_1 \rho_2} \quad (S1),$$

where ρ_i and ω_i are the density and mass fractions of the single components, respectively. Numbers 1, 2 and 3 correspond to PANI, CHT and PVA, respectively. The density of PANI (in its base form) was 1.24 g/cm^3 [6], CHT and PVA are 0.7 and 1.29 g/cm^3, respectively (see section 2.1 above).

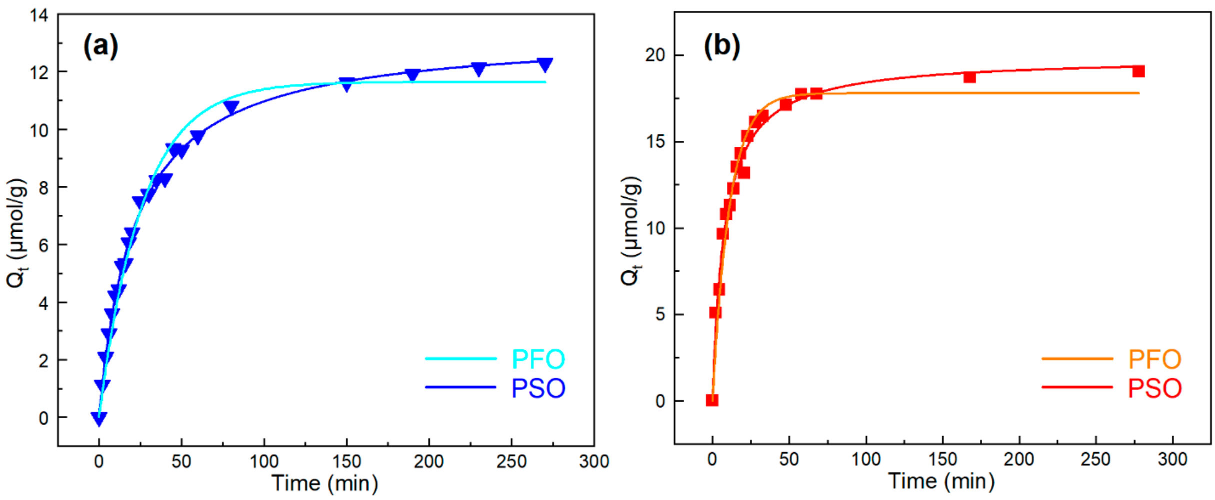

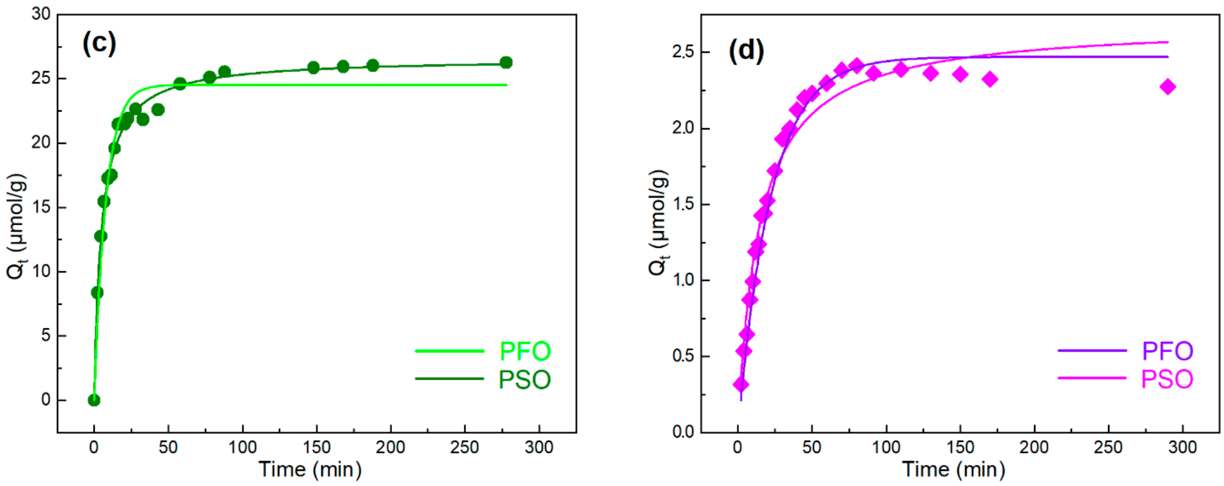

Figure S4. Fitting lines for (**a**) CHP25-PVA, (**b**) CHP50-PVA, (**c**) CHP75-PVA and (**d**) pristine CHT MB kinetic uptake according to the PFO and PSO models. The error bars were determined using OriginLab 2019 software (see Table S5).

Table S5. Error bars for the adsorption experiments shown in Figure S4.

Sample	**Model / Parameters**	**Pseudo-First Order**	**Pseudo-second Order**
	Equation	$y = q(1 - e^{-kx})$	$y = \frac{q^2kx}{1+qkx}$
	Plot	$Q_t = f(t)$	$Q_t = f(t)$
CHP25-PVA	q	11.64 ± 0.20	13.36 ± 0.11
	k	0.03821 ± 0.00174	(3.431 ± 0.115) × 10^{-3}
	Reduced Chi-Sqr	1.979 × 10^{-7}	3.231 × 10^{-8}
	R-Square (COD)	0.9859	0.9977
	Adj. R-Square	0.9852	0.9976
CHP50-PVA	q	17.78 ± 0.37	19.87 ± 0.30
	k	0.09079 ± 0.00621	(6.353 ± 0.465) × 10^{-3}
	Reduced Chi-Sqr	7.738 × 10^{-7}	2.754 × 10^{-7}
	R-Square (COD)	0.9727	0.9903
	Adj. R-Square	0.9710	0.9897
CHP75-PVA	q	24.52 ± 0.43	26.59 ± 0.23
	k	0.12785 ± 0.00988	(7.478 ± 0.403) × 10^{-3}
	Reduced Chi-Sqr	1.896 × 10^{-6}	3.229 × 10^{-7}
	R-Square (COD)	0.9587	0.9930
	Adj. R-Square	0.9565	0.9926
CHT	q	2.47 ± 0.003	2.69 ± 0.06
	k	0.04473 ± 0.00039	0.02591 ± 2.64

Reduced Chi-Sqr	7.495×10^{-9}	1.408×10^{-8}
R-Square (COD)	0.9531	0.9701
Adj. R-Square	0.9531	0.9688

Figure S5. Batch adsorption experiment that illustrates decolorization of FL solutions by the PANI-based adsorbent at pH 7: (**a**) initial solutions (before adsorption); (**b**) after 24 h (after adsorption). The vials numbered 501–515 indicate that this experiment was conducted for CHP25-PVA doped (#5) in the range of FL concentrations 20 to 500 µM (#01 to #15).

Table S6. Water vapor adsorption parameters of the doped and undoped composites in their film form.

	Adsorption				Desorption			
	ω_{max} (‰)	a	b	R^2	ω_{max} (‰)	c	d	R^2
CHP25-PVA doped	267	1.77	3.92	0.996	267	0.0233	−0.0201	0.999
CHP50-PVA doped	308	1.71	4.13	1.000	308	0.0207	−0.0179	0.997
CHP75-PVA doped	336	1.25	4.68	0.993	336	0.0205	−0.0180	0.998
CHP25-PVA	224	1.91	3.57	0.993	224	0.0247	−0.0208	0.998
CHP50-PVA	230	1.09	4.46	0.999	230	0.0252	−0.0215	0.998
CHP75-PVA	241	1.53	4.05	0.993	241	0.0237	−0.0201	0.998

Table S7. Current-voltage parameters for the I-V curves of samples in their film form. .

	Film	β	K (µA·cm^{-2}·V$^{-\beta}$)	R^2
	CHP25-PVA70 doped	1.26	0.0122	0.998
(a)	CHP50-PVA70 doped	2.44	0.000350	0.999
	CHP75-PVA70 doped	1.85	0.00193	0.999

	CHP25-PVA50 doped	1.19	2.14	0.998
(b)	CHP50-PVA50 doped	1.08	1.63	0.999
	CHP75-PVA50 doped	0.990	0.919	0.998

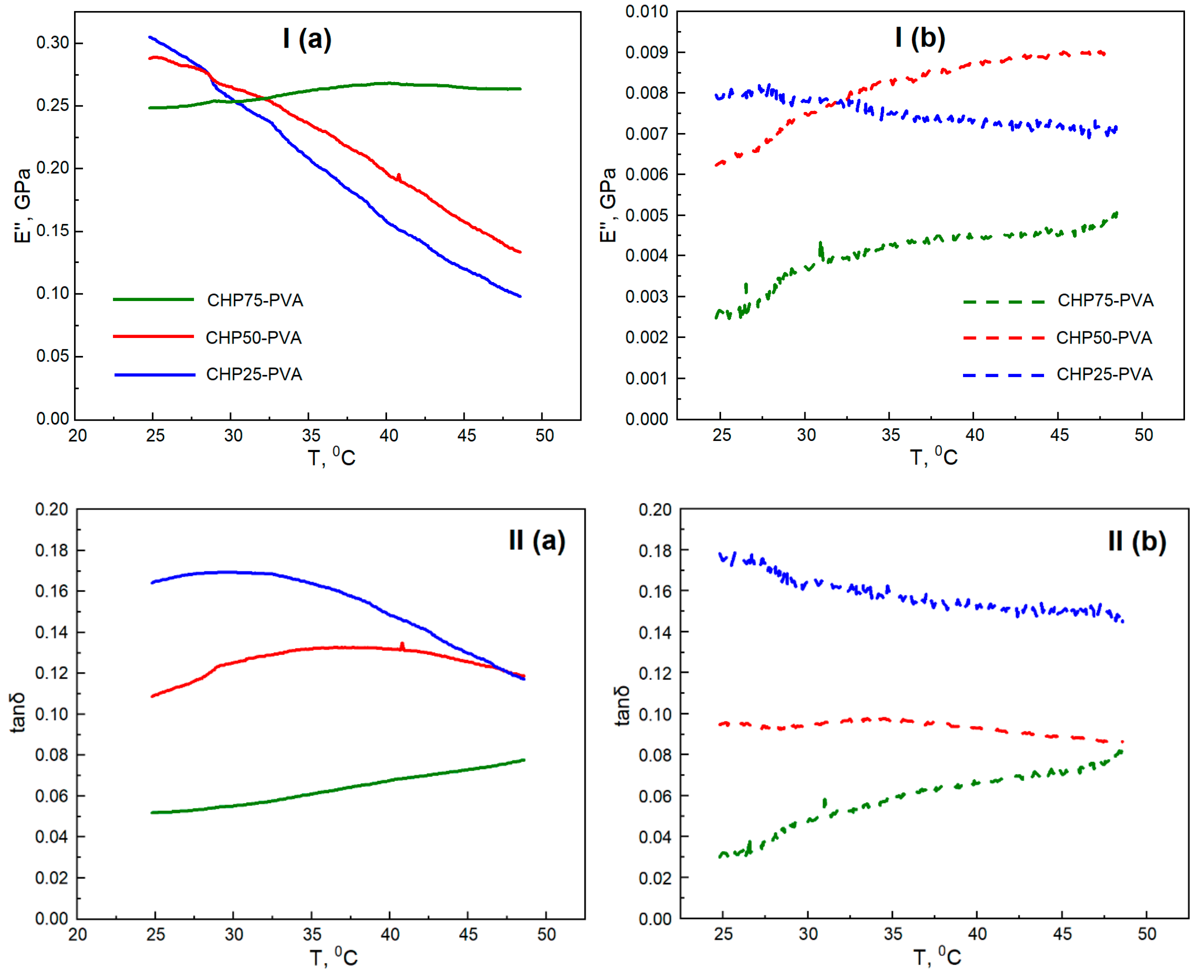

Figure S6. DMA mechanical properties of the base-neutralized films in their (**a**) dry, and (**b**) wet state: I – loss modulus; II – tan delta.

References

1. Mahaninia, M.H.; Wilson, L.D. Modular Cross-Linked Chitosan Beads with Calcium Doping for Enhanced Adsorptive Uptake of Organophosphate Anions. *Ind. Eng. Chem. Res.* **2016**, *55*, 11706–11715.
2. Mohamed, M.H.; Dolatkhah, A.; Aboumourad, T.; Dehabadi, L.; Wilson, L.D. Investigation of templated and supported polyaniline adsorbent materials. *RSC Adv.* **2015**, *5*, 6976–6984.
3. Do Nascimento, G.M., Spectroscopy of Polyaniline Nanofibers. Available Online: https://www.intechopen.com/books/nanofibers/spectroscopy-of-polyaniline-nanofibers (access on 6 February 2020).
4. Trchova, M.; Stejskal, J. Polyaniline: The Infrared Spectroscopy of Conducting Polymer Nanotubes (IUPAC Technical Report). *Pure Appl. Chem.* **2011**, *83*, 1803–1817.

5. Mansur, H.S.; Sadahira, C.M.; Souza, A.N.; Mansur, A.A.P. FTIR Spectroscopy Characterization of Poly (Vinyl Alcohol) Hydrogel with Different Hydrolysis Degree and Chemically Crosslinked with Glutaraldehyde. *Mater. Sci. Eng. C* **2008**, *28*, 539–548.
6. Stejskal, J.; Gilbert, R.G. Polyaniline. Preparation of a Conducting Polymer (IUPAC Technical Report). *Pure Appl. Chem.* **2002**, *74*, 857–867.